J Nanopart Res (2015) 17:474
DOI 10.1007/s11051-015-3287-8

BRIEF COMMUNICATION

Electro-oxidation of methanol in alkaline conditions using Pd–Ni nanoparticles prepared from organometallic precursors and supported on carbon vulcan

**A. Manzo-Robledo · Natália J. S. Costa · K. Philippot ·
Liane M. Rossi · E. Ramírez-Meneses · L. P. A. Guerrero-Ortega ·
S. Ezquerra-Quiroga**

Received: 26 July 2015 / Accepted: 30 November 2015 / Published online: 9 December 2015

Abstract Oxidation of low-molecular weight alcohols as energy sources using metal nanoparticles has attracted considerable interest for use as a power source in portable electronic devices. In this work, a series of mono- and bimetallic nanoparticles based on palladium and nickel (Pd, $Pd_{90}Ni_{10}$, $Pd_{50}Ni_{50}$, $Pd_{10}Ni_{90}$, and Ni) have been synthesized from organometallic precursors, namely tris(dibenzylideneacetone) dipalladium(0), $Pd_2(dba)_3$, and bis(1,5-cyclooctadiene)nickel(0), $Ni(cod)_2$. Well-defined metal particles in the nanometric scale from 4.2 to 6.3 nm were observed by transmission electron microscopy. The as-prepared nanoparticles were mixed with a carbon Vulcan matrix (10 % wt. of the catalyst in turn) for investigation as electrocatalysts in methanol oxidation reaction (MOR) in alkaline conditions. The *i–E* profiles from cyclic voltammetry for the monometallic systems indicated a redox process attributed only to palladium or nickel, as expected. With the bimetallic nanomaterials, the redox process and the *i–E* characteristics are functions of the amount of nickel associated to palladium. From a fundamental point of view, it has been established that the OH ions' interfacial interaction and the MOR kinetics are affected by the presence of nickel (decreasing the faradic current) as supported by the current versus potential profiles obtained as a function of methanol concentration and with temperature variation.

Keywords Methanol oxidation · Electrocatalysis · Fuel cell · Anode catalyst · Colloidal catalyst precursor

Introduction

Direct alcohol fuel cells (DAFCs) have attracted considerable attention because of their interest as alternative power sources for vehicles and portable electronic devices (Badwal et al. 2015; Zhang et al. 2015, Hansen 2015). The use of low-molecular weight alcohols such as methanol or ethanol as energy sources has numerous advantages, since for example these compounds can be easily handled, stored, and

A. Manzo-Robledo (✉) · L. P. A. Guerrero-Ortega
Laboratorio de Electroquímica y Corrosión, Escuela Superior de Ingeniería Química e Industrias Extractivas-IPN, UPALM, 07738 Mexico, D.F., Mexico
e-mail: amanzor@ipn.mx

N. J. S. Costa · L. M. Rossi
Instituto de Química, Universidade de São Paulo, Av. Professor Lineu Prestes, 748, São Paulo, SP 05508-000, Brazil

N. J. S. Costa · K. Philippot
Laboratoire de Chimie de Coordination, CNRS, LCC, 205, Route de Narbonne, BP 44099F-31077, Toulouse, France

E. Ramírez-Meneses · S. Ezquerra-Quiroga
Departamento de Ingeniería y Ciencias Químicas, Universidad Iberoamericana, Prolongación Paseo de la Reforma 880, Lomas de Santa Fe, 01219 Mexico, D.F, Mexico

transported. Nevertheless, there are limitations related to the application of DAFCs, including the high cost of the final devices, low levels of electrocatalytic activity, and reduced durability. Up to now, the most common electrocatalysts used in DAFCs contain platinum and palladium alloys because of the outstanding electrocatalytic activity of these materials. However, Pt cannot be used for large-scale applications owing to its high cost and toxicity by carbon monoxide (CO). Additionally, alkaline direct alcohol fuel cells present an important advantage having a basic electrolyte membrane which implies reaction kinetics of both the alcohol anodic oxidation and oxygen cathodic reduction faster than in acidic media, making it possible to use Pt-free metal catalysts (Xu et al. 2008; Jiang et al. 2010; Estudillo-Wong et al. 2013). Thus, alternative materials are needed (Shen and Xu 2006) and today researches are largely focused on Pd-based electrocatalysts for fuel cells. Moreover, it has been found that by allowing a second metal such as Fe, Co, Au, or Ni, the d-band of Pd can be modified (Su et al. 2013). For these reasons, bimetallic catalysts with alloy structures are an important research topic for application in low-molecular weight alcohols such as methanol or ethanol due to their enhanced activity and stability, different from those of the monometallic components (Su et al. 2013; Demirci 2007; Manzo-Robledo et al. 2003).

Metal nanoparticles display a considerable interest as catalysts in organic and inorganic reactions, as electrocatalysts in fuel cells or materials with novel electronic, optical, and magnetic properties. Consequently, many research works are dedicated to the development of synthetic methods for the size- and shape-selective preparation of noble metal nanoparticles (Roucoux et al. 2002; Durán Pachón and Rothenberg 2008; Tao and Habas 2008; Niu and Xu 2011; Chen and Liu 2011; Lu and Yin 2012; Sastry et al. 2005). Comparisons of the effect of synthesis method on the catalytic performance of metal nanoparticles when used as electrocatalysts for methanol or ethanol electro-oxidation in alkaline media have been reported (Zhao et al. 2014; Lin et al. 2009; Antolini 2007; Bandarenka and Koper 2013; Yu et al. 2010; Park and Sung 2006). Conventional chemical methods to obtain Pd or PdNi nanoparticles are based on the chemical reduction of metal transition salts such as $PdCl_2$, $Pd(NO_3)_2$, $NiCl_2$, $NiSO_4$, and $Ni(NO_3)_2$ using $NaBH_4$ as a reducing agent (Xu et al. 2007; Zhang et al. 2011; Amin et al. 2014a, b; Yang et al. 2014; Awasthi and Anindita 2010; Shen et al. 2010; Jin et al. 2012; Zhao et al. 2010). Alternative syntheses have been reported for the same precursors, like modified polyol reduction process in the presence of ethylene glycol or glycerol as reducing agents (Cai et al. 2013; Li et al. 2015). Other reducing agents such as hydrazine, formic acid, or dihydrogen have also been employed (Guo et al. 2012; Liu et al. 2009; Wei et al. 2011; Su et al. 2013). An interesting method that includes cathodic deposition using hydrogen dynamic bubble template allowed obtaining Pd and PdNi nanostructures ($\sim$10 nm) having three-dimensional hierarchical pores of interconnected dendrite walls (Li et al. 2013). An alternative method includes a conventional electrodeposition of Pd spherical nanostructures in the range of 140–350 nm and PdNi nanostructures of 10–26 nm in diameter (Yi et al. 2013). A similar method employing electrodeposition followed by galvanic replacement allowed obtaining spherical porous aggregates of 58 nm in size (Hosseini et al. 2013). A modified polyol process based on $Pd(acac)_2$ as a precursor and 1,2-hexadecanediol as a reducing agent led to the formation of Pd nanoflowers (Yin et al. 2009). $Pd(acac)_2$ precursor has been also used in a modified solution phase-based nanocapsule method in the presence of lithium triethylborohydride to generate Pd nanoparticles of 2–2.3 nm in size (Zhang et al. 2011). A non-conventional but still interesting method is the melt spinning technique and subsequent dealloying of $Al_{75}Pd_{10}Ni_{15}$ precursor in 20 wt% NaOH to prepare $Pd_{40}Ni_{60}$ nanorods (Qi et al. 2011). Furthermore, the electron beam irradiation method using $Pd(NO_3)_2 \cdot 2H_2O$ as a precursor and solvated electrons and $\dot{H}$ radicals as reducing agents has been effectively used to prepare spherical Pd nanoparticles of 7.1–7.5 nm in size (Napoleão Geraldes et al. 2013).

Another advantageous chemical preparation method is based on the use of organometallic precursors. This method was developed by Chaudret for the synthesis of transition metal nanoparticles (Amiens et al. 2013). The main advantage of using such metal precursors is their facile decomposition that can be achieved in organic solution, in the presence of different stabilizing agents and under mild conditions. In this way, the control of the particles' size, shape, and surface state can be achieved which facilitates the generation of monodisperse systems. Bimetallic nanoparticles with variable metal ratios can also be prepared by this organometallic approach (Costa et al. 2014). For instance, Ni, Pt, and Ni_xPt ($x = 1, 2, 3$) nanoparticles stabilized by hexadecylamine (HDA) were prepared and evaluated as electrocatalysts for the hydrogen evolution reaction (HER). The presence of donor ligands such as amines did not block electron transfer for the HER reaction, and excellent electrocatalytic activity on HER was obtained (Domínguez-Crespo et al. 2009, 2012). Moreover, the mean diameter of the Ni_xPt nanostructures in the range of 2–5 nm appeared to correlate with the platinum amount and the interaction between the metallic nanoparticles and stabilizer HDA (Domínguez-Crespo et al. 2012). The composition of NiPt catalysts influenced strongly the electrocatalytic activity for HER.

In continuation of our prior studies on the electrochemical properties of bimetallic nanoparticles, here we further explore the interest of organometallic Pd, Ni, and PdNi nanoparticles containing different Pd:Ni molar ratios with the aim to determine how this metal composition can affect the catalytic performance of such nanomaterials in methanol oxidation reaction under alkaline conditions.

Experimental section

Synthesis of metal nanoparticles

The bimetallic NiPd nanoparticles with different Ni:Pd molar ratios (50:50, 90:10, and 10:90) in the presence of an excess of hexadecylamine (HDA) were prepared under inert atmosphere using vacuum line techniques by co-decomposition of tris(dibenzylideneacetone)dipalladium(0), $Pd_2(dba)_3$, and bis(1,5-cyclooctadiene)nickel(0), $Ni(cod)_2$, as previously reported (Costa et al. 2014). The as-prepared catalyst powders were mixed with carbon Vulcan in order to obtain supported active material (10 % wt. Pd_xNi_y/C).

TEM analysis

The size and morphology of the obtained nanostructures were determined using a JEOL JEM 2010 transmission electron microscope. TEM samples were prepared by dropping each crude colloidal solution onto a carbon-covered copper grid.

Electrode preparation and electrochemical experiments

The electrochemical measurements were performed potentiostatically (Versastat 3) in a three-electrode standard electrochemical cell. A carbon rod and saturated Calomel electrode (SCE) were used as counter (CE) and reference electrodes, respectively. A glassy carbon (GC) disk electrode with 4 mm in diameter, polished to a mirror-like finish with a 0.05 μm alumina suspension before each experiment, was used as the substrate for the catalyst ink. The ink was prepared by dispersing 4.0 mg of electrocatalyst in 0.1 % vol. solution (5 wt % Nafion) in ultrasound bath for 30 min. The same procedure was carried out for the preparation of the carbon Vulcan ink free of catalyst. An aliquot of 6.3 μL of this ink was deposited onto the GC surface and dried under argon atmosphere. The methanol concentration was xM MetOH + 0.5 M NaOH ($x = 0.01$ M, 0.1 M, 0.5 M and 1 M). The temperature varied from 20 to 60 °C, using a solution of 0.5 M methanol and 0.5 M NaOH. For all experiments, gas argon was used to eliminate oxygen from electrolyte. All reagents were used without further purification.

Results and discussion

Characterization of NiPd nanoparticles

Pd, $Pd_{90}Ni_{10}$, $Pd_{50}Ni_{50}$, $Pd_{10}Ni_{90}$, and Ni nanoparticles were obtained from the decomposition of $Pd_2(dba)_3$ and $Ni(cod)_2$ precursors under dihydrogen atmosphere in the presence of 10 molar equivalents of HDA in toluene. Well-dispersed, semi-spherical, and regular size metal nanoparticles with average sizes of Pd (5.4 nm), $Pd_{90}Ni_{10}$ (6.1 nm), $Pd_{50}Ni_{50}$ (4.2 nm), $Pd_{10}Ni_{90}$ (5.1 nm), and Ni (6.3 nm) were previously characterized by TEM (Costa et al. 2014). Additional TEM characterization is shown in Fig. 1, and the average particle size is in the order Ni > $Pd_{10}Ni_{90}$ > Pd > $Pd_{90}Ni_{10}$ > $Pd_{50}Ni_{50}$. As previously discussed regarding Pd, Pt, and Ni nanoparticles (Ramírez et al. 2004; Costa et al. 2014; Ramírez et al. 2007; Cordente et al. 2001), the large amount of HDA allows good stabilization of the nanoparticles. The purification of the nanoparticles was performed by repeated cycles of precipitation with cold pentane in an ice bath;

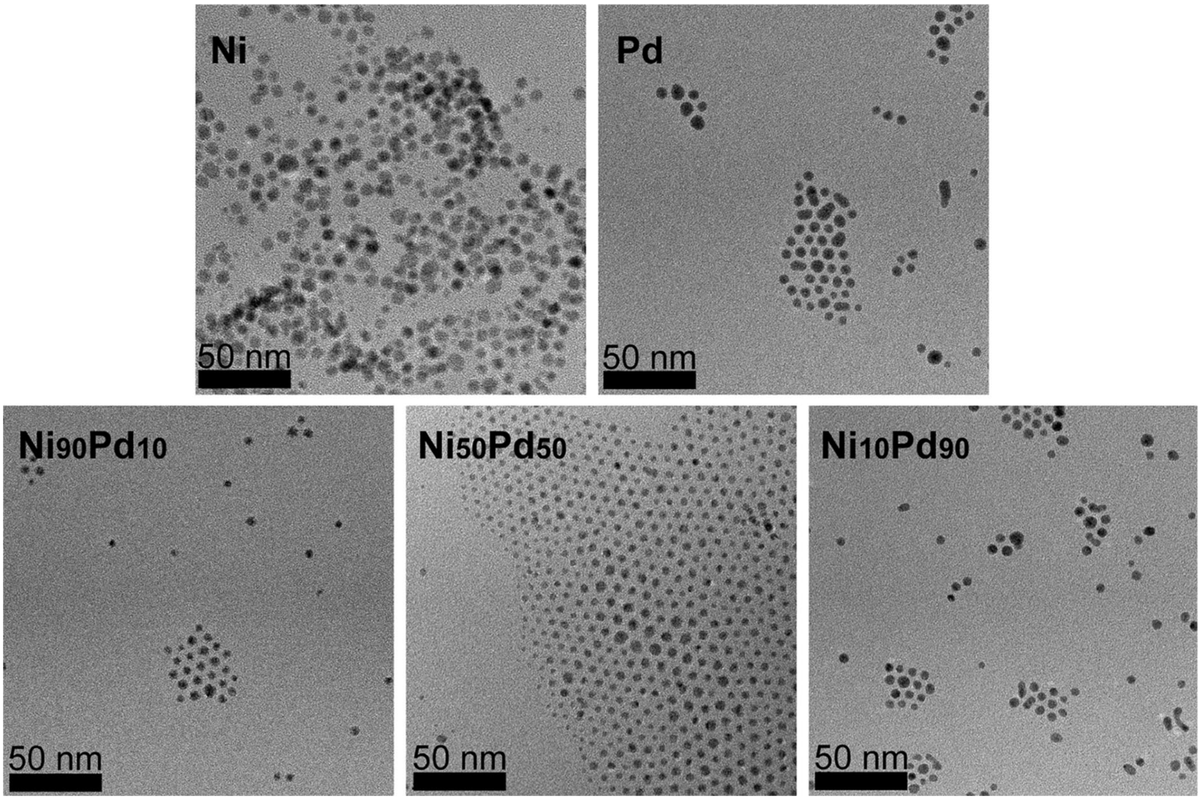

Fig. 1 Size and morphology of the as-prepared nanoparticles stabilized by HDA: Ni, $Ni_{90}Pd_{10}$, $Ni_{50}Pd_{50}$, $Ni_{10}Pd_{90}$, and Pd

however, the excess of HDA was not completely removed due to the simultaneous precipitation of HDA. When the purification was performed at room temperature, a more efficient removal of HDA was achieved, but it also decreases the amount of nanoparticles recovered. The Pd:Ni molar ratio was determined by ICP OES and it is very close to the theoretical ratio for all the bimetallic nanoparticles (0.9:9.1; 4.9:5.1, and 8.9:1.1 for $Pd_{10}Ni_{90}$, $Pd_{50}Ni_{50}$, and $Pd_{90}Ni_{10}$, respectively) (Costa et al. 2014). The excess of HDA did not allow us to obtain a description of the Pd and Ni metal domain distribution in the isolated nanoparticles by chemical mapping using the STEM-XEDS technique. The bimetallic nanostructure of the PdNi nanoparticles prepared by the co-decomposition of the organometallic precursors could be assessed after their immobilization on silica as presented in (Costa et al. 2014). Analysis of many compositional maps revealed segregation of nickel at the nanoparticle surface, which was also in agreement with the XPS results, showing the presence of nickel oxide on the nanoparticles' surface (Costa et al. 2014). The segregation of Pd and Ni domains is expected in nickel−palladium disordered alloys because of the mismatch of the atomic size of Ni and Pd.

Electrochemical analysis

Figure 2 reports the current versus potential profiles obtained by cyclic voltammetry at a scan rate of 50 mV s^{-1} in alkaline conditions for the samples in this study. It is important to note that the shapes of these curves are very different for monometallic palladium (Fig. 2a) and nickel (Fig. 2c) nanoparticle systems, representing the redox process corresponding only to Pd or Ni, as expected. During surface polarization at the intermediate bimetallic nanoparticle materials, named Pd_x–Ni_y/C (Fig. 2b), some differences can be observed: (i) the intensity of the typical peak of Pd in alkaline conditions decreases as a consequence of the presence of nickel at 10 and 50 %; (ii) at 90 % of nickel, such a peak exhibits an onset to

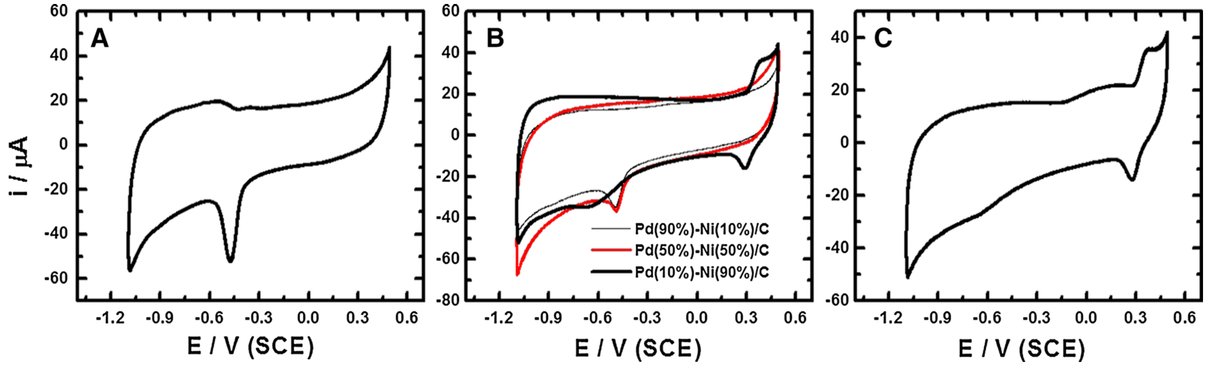

Fig. 2 *i–E* characteristics obtained during cyclic voltammetry at 50 mV s^{-1} in 0.5 M NaOH solution. Starting potential at open circuit toward positive direction. **a** Pd/C, **b** Pd_x–Ni_y/C, and **c** Ni/C

more negative potentials; and (iii) typical peaks of nickel are only visible at $Pd_{10}Ni_{90}$/C.

On the other hand, typical current–potential characteristics showing methanol oxidation reaction (MOR) into carbon dioxide were observed during polarization at 5 mV s^{-1} using cyclic voltammetry in 0.5 M NaOH and different methanol concentrations for all catalysts; for simplicity, Fig. 3 shows the profiles obtained at Pd/C, whereas the inset of this figure shows the current–potential characteristic of a palladium electrode in a solution free of methanol (curve (a)) and carbon Vulcan deposited on the surface of glassy carbon electrode (curve (b)). As can be observed, the carbon Vulcan ink (prepared as mentioned in the experimental section) deposited onto glassy carbon did not affect the corresponding methanol oxidation in the potential-window interval (ca. −0.6 to 0.0 V/SCE). On the other hand, it is well known that Ni possesses inferior electrochemical activity than Pd; however, it is also expected that nanostructured bimetallic alloys might combine the properties of the individual constituents due to some kind of composition and reorganization at nanometric scale. Then for the Pd-Ni material, the accumulation of nickel species on the surface is possible (Costa et al. 2014; Tong et al. 2012; Wu et al. 2011); as a consequence, the electro-induced interfacial reaction might be altered (vide infra). Thus, although it is possible to assume that methanol oxidation is carried out, the magnitude of the current increases as a function of palladium content, as can be discerned from Fig. 4. In this figure, the faradic current variation as a function of methanol concentration is depicted and is in the order Pd > $Pd_{90}Ni_{10}$ > $Pd_{50}Ni_{50}$ > $Pd_{10}Ni_{90}$ > Ni, within experimental error. However, with a low methanol concentration, this behavior is altered as nickel sites could interact in a different way when methanol is better distributed (dilute) in the vicinity of electrode–electrolyte interface in order to interact with the OH ions. This behavior was also verified with respect to temperature at constant concentration of methanol as shown in Fig. 5; then, the activation energy for the MOR is altered in temperature by the material in turn increasing the interaction in the catalyst active sites, and decreasing as a function of

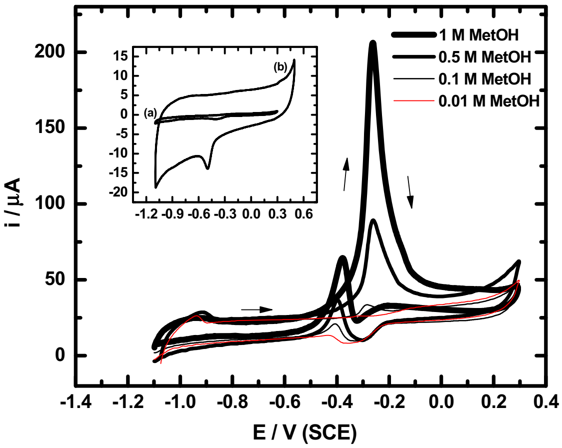

Fig. 3 Typical profiles corresponding to methanol oxidation in alkaline conditions, presented here for Pd/C. The observed peaks are assigned to the CO_2 formation at the electrode interface. The *inset* shows *a* the current–potential (*i–E*) profile for Pd in a solution free of methanol and *b* the profile (*i–E*) corresponding to carbon Vulcan (free of catalyst) deposited onto glassy carbon. Supporting electrolyte is 0.5 M NaOH; starting potential was fixed at −1.1 V in the positive direction; scan rate is 5 mV s^{-1}

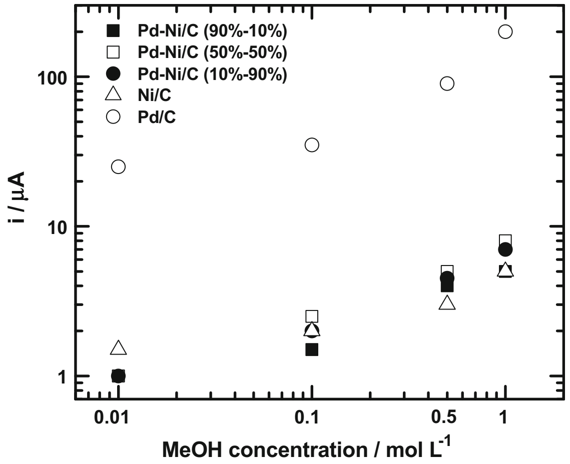

Fig. 4 Current versus concentration variation profiles with respect to Ni loading during methanol oxidation reaction. Data were obtained at maximum current during the positive-going scan. The scan rate was fixed at 5 mV s^{-1}

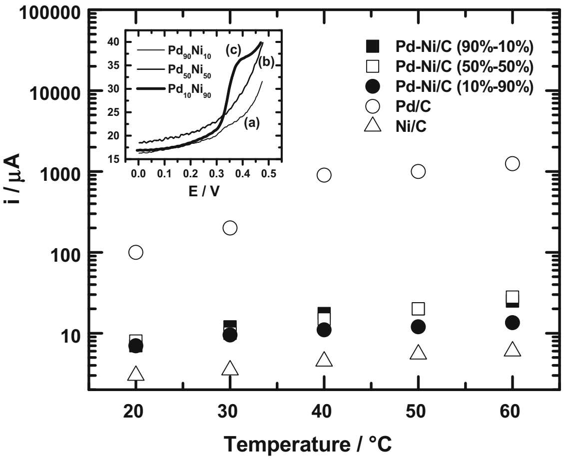

Fig. 5 Current versus temperature variation profiles with respect to Ni loading during the methanol oxidation reaction. Data were obtained at maximum current during the positive-going scan. The scan rate was fixed at 5 mV s^{-1}. *Inset* current–potential profiles in the OER zone

palladium loading (Estudillo-Wong et al. 2013). From these results, we can assume that nickel added to palladium in the nanoparticles influences the OH–methanol surface interaction and decreases the activity for alcohol oxidation by modifying the reaction selectivity toward, probably, the oxygen evolution reaction (OER) (Estudillo-Wong et al. 2013). From this assumption, the OER anodic current increases as nickel content increases for the bimetallic $Pd_{90}Ni_{10}$ and $Pd_{50}Ni_{50}$ (see curves (a) and (b) in the inset of Fig. 5) until reaching the oxidation of nickel at $Pd_{10}Ni_{90}$ and then inhibiting the evolution of oxygen as a secondary reaction (see curve (c) in the inset of Fig. 5). Therefore, during polarization in presence of alcohol, OH ions are selectively adsorbed on nickel sites, promoting a major conversion toward the OER (at more anodic potentials) instead of methanol oxidation at high and moderate Ni concentration and in the catalyst free of palladium. This last assumption might be linked with the mechanism of formation of the bimetallic nanoparticles from $Ni(cod)_2$ and $Pd_2(dba)_3$ since under experimental conditions (with dihydrogen) $Pd_2(dba)_3$ decomposes to generate Pd(0) nanoparticles which may then catalyze the decomposition of $Ni(cod)_2$ to produce bimetallic nanoparticles containing palladium at the core and an excess of nickel atoms on the surface (Costa et al. 2014; Cordente et al. 2001; Ramírez et al. 2004).

Conclusions

The methanol oxidation reaction was investigated using Pd–Ni-based nanoparticles ranging from 4.2 to 6.3 nm in size prepared from organometallic precursors. Redox characteristics including Pd to Ni were observed during cyclic voltammetry experiments in the alkaline environment. It was found that methanol oxidation is possible in all set of catalysts evaluated. However, for this case of study, the presence of nickel-(oxide) species and the possible formation of a core–shell system associated with palladium induce electronic and structural modification during the transition from nickel to palladium that modifies the OH ions' surface adsorption interaction, reaction kinetic performance, and the selectivity conversion toward the interfacial coupled OER–MOR in the alkaline environment.

Acknowledgments The authors wish to acknowledge the financial support provided by SIP and IPN-CONACyT (projects 160333 and 157613), Universidad Iberoamericana 0053 project, SNI-CONACyT, CAPES, FAPESP, and the CNRS. The authors also thank V. Collière (UPS-TEMSCAN) for TEM analysis. The research was conducted in the framework of the "French-Mexican International Laboratory (LIA) LCMMC" and "International Cooperation Program CAPES-COFECUB (Grant 695/10)."

References

Amiens C, Chaudret B, Ciuculescu-Pradines D, Collière V, Fajerwerg K, Fau P, Kahn M, Maisonnat A, Soulantica K, Philippot K (2013) Organometallic approach for the synthesis of nanostructures. New J Chem 37:3374–3401

Amin RS, Abdel Hameed RM, El-Khatib KM (2014a) Microwave heated synthesis of carbon supported Pd, Ni and Pd–Ni nanoparticles for methanol oxidation in KOH solution. Appl Catal B 148–149:557–567

Amin RS, Abdel Hameed RM, El-Khatib KM, Elsayed YM (2014b) Electrocatalytic activity of nanostructured Ni and Pd–Ni on Vulcan XC-72R carbon black for methanol oxidation in alkaline medium. Int J Hydrog Energy 39:2026–2041

Antolini E (2007) Catalysts for direct ethanol fuel cells. J Powder Sources 170:1–12

Awasthi R, Anindita RN (2010) Synthesis and characterization of nano structured Pd-Ni and Pd–Ni–C composites towards electrooxidation of alcohols. Open Catal J 3:70–78

Badwal SPS, Giddey S, Kulkarni A, Goel J, Basu S (2015) Direct ethanol fuel cells for transport and stationary applications—a comprehensive review. Appl Energy 145:80–103

Bandarenka AS, Koper MTM (2013) Structural and electronic effects in heterogeneous electrocatalysis: toward a rational design of electrocatalysts. J Catal 308:11–24

Cai J, Huang Y, Guo Y (2013) Bi-modified Pd/C catalyst via irreversible adsorption and its catalytic activity for ethanol oxidation in alkaline medium. Electrochim Acta 99:22–29

Chen HM, Liu R-S (2011) Architecture of metallic nanostructures: synthesis strategy and specific applications. J Phys Chem C 115:3513–3527

Cordente N, Respaud M, Senocq F, Casanove MJ, Amiens C, Chaudret B (2001) Synthesis and magnetic properties of nickel nanorods. Nano Lett 1:565–568

Costa NJS, Guerrero M, Collière V, Teixeira-Neto E, Landers R, Philippot K, Rossi LM (2014) Organometallic preparation of Ni, Pd, and NiPd nanoparticles for the design of supported nanocatalysts. ACS Catal 4:1735–1742

Demirci UB (2007) Theoretical means for searching bimetallic alloys as anode electrocatalysts for direct liquid-feed fuel cells. J Power Sources 173:11–18

Domínguez-Crespo MA, Ramírez-Meneses E, Montiel-Palma V, Torres-Huerta AM, Dorantes Rosales H (2009) Synthesis and electrochemical characterization of stabilized nickel nanoparticles. Int J Hydrog Energy 34:1664–1676

Domínguez-Crespo MA, Ramírez-Meneses E, Torres-Huerta AM, Garibay-Febles V, Philippot K (2012) Kinetics of hydrogen evolution reaction on stabilized Ni, Pt and Ni–Pt nanoparticles obtained by an organometallic approach. Int J Hydrog Energy 37:4798–4811

Durán Pachón L, Rothenberg G (2008) Transition-metal nanoparticles: synthesis, stability and the leaching issue. Appl Organometal Chem 22:288–299

Estudillo-Wong LA, Vargas-Gómez AM, Arce-Estrada EM, Manzo-Robledo A (2013) TiO_2/C composite as a support for Pd-nanoparticles toward the electrocatalytic oxidation of methanol in alkaline media. Electrochim Acta 112:164–170

Guo P, Wei Z, Ye W, Qin W, Wang Q, Guo X, Lu C, Zhao XS (2012) Preparation and characterization of nanostructured Pd with high electrocatalytic activity. Colloids Surf A 395:75–81

Hansen JB (2015) Fuel processing for fuel cells and power to fuels as seen from an industrial perspective. J Catal 328:280–296

Hosseini MG, Abdolmaleki M, Ashrafpoor S (2013) Methanol electro-oxidation on a porous nanostructured Ni/Pd-Ni electrode in alkaline media. Chin J Catal 34:1712–1719

Jiang L, Hsu A, Chu D, Chen R (2010) Ethanol electro-oxidation on Pt/C and PtSn/C catalysts in alkaline and acid solutions. Int J Hydrog Energy 35:365–372

Jin C, Sun X, Chen Z, Dong R (2012) Electrocatalytic activity of PdNi/C catalysts for allyl alcohol oxidation in alkaline solution. Mater Chem Phys 135:433–437

Li R, Mao H, Zhang J, Huang T, Yu A (2013) Rapid synthesis of porous Pd and PdNi catalysts using hydrogen bubble dynamic template and their enhanced catalytic performance for methanol electrooxidation. J Power Sources 241:660–667

Li Z, Lu H, Li Q, Zhao XS, Guo P (2015) Template synthesis of palladium nanotubes and their electrocatalytic properties. Colloids Surf A 464:129–133

Lin Y-C, Chou H-L, Tsai M-C, Hwang B-J, Subramanyam L, Lee Y-C, Chen C-I (2009) Combined experimental and theoretical investigation of nanosized effects of Pt catalyst on their underlying methanol electro-oxidation activity. J Phys Chem C 113:9197–9205

Liu Z, Zhang X, Hong L (2009) Physical and electrochemical characterizations of nanostructured Pd/C and PdNi/C catalysts for methanol oxidation. Electrochem Commun 11:925–928

Lu Z, Yin Y (2012) Colloidal nanoparticle clusters: functional materials by design. Chem Soc Rev 41:6874–6887

Manzo-Robledo A, Boucher A-C, Pastor E, Alonso-Vante N (2003) Electro-oxidation of carbon monoxide and methanol on carbon-supported Pt–Sn nanoparticles: a DEMS study. Fuel Cells 2:109–116

Napoleão Geraldes A, Furtunato da Silva D, Segura Pino E, Martins da Silva JC, Brambilla de Souza RF, Hammer P, Vitório Spinacé E, Oliveira Neto A, Linardi M, Coelho dos Santos M (2013) Ethanol electro-oxidation in an alkaline medium using Pd/C, Au/C and PdAu/C electrocatalysts prepared by electron beam irradiation. Electrochim Acta 111:455–465

Niu W, Xu G (2011) Crystallographic control of noble metal nanocrystals. Nano Today 6:265–285

Park K-W, Sung Y-E (2006) Design of nanostructured electrocatalysts for direct methanol fuel cells. J Ind Eng Chem 12:165–174

Qi Z, Geng H, Wang X, Zhao C, Ji H, Zhang C, Xu J, Zhang Z (2011) Novel nanocrystalline PdNi alloy catalyst for methanol and ethanol electro-oxidation in alkaline media. J Power Sources 196:5823–5828

Ramírez E, Jansat S, Philippot K, Lecante P, Gomez M, Masdeu-Bulto A, Chaudret B (2004) Influence of organic ligands on the stabilization of palladium nanoparticles. J Organometallic Chemistry 689:4601–4610

Ramírez E, Erades L, Philippot K, Lecante P, Chaudret B (2007) Shape control of platinum nanoparticles. Adv Funct Mater 17:2219–2228

Roucoux A, Schulz J, Patin H (2002) Reduced transition metal colloids: a Novel family of reusable catalysts? Chem Rev 102:3757–3778

Sastry M, Swami A, Mandal S, Selvakannan PR (2005) New approaches to the synthesis of anisotropic, core–shell and hollow metal nanostructures. J Mater Chem 15:3161–3174

Shen PK, Xu C (2006) Alcohol oxidation on nanocrystalline oxide Pd/C promoted electrocatalysts. Electrochem Commun 8:184–188

Shen SY, Zhao TS, Xu JB, Li YS (2010) Synthesis of PdNi catalysts for the oxidation of ethanol in alkaline direct ethanol fuel cells. J Power Sources 195:1001–1006

Su P-C, Chen H-S, Chen T-Y, Liu C-W, Lee C-H, Lee J-F, Chan T-S, Wang K-W (2013) Enhancement of electrochemical properties of Pd/C catalysts toward ethanol oxidation reaction in alkaline solution through Ni and Au alloying. Int J Hydrog Energy 38:4474–4482

Tao AR, Habas S (2008) Shape control of colloidal metal nanocrystals. Small 4:310–325

Tong X, Qin Y, Guo X, Moutanabbir O, Ao X, Pippel E, Zhang L, Knez M (2012) Enhanced catalytic activity for methanol electro-oxidation of uniformly dispersed nickel oxide nanoparticles-carbon nanotube hybrid materials. Small 8:3390–3395

Wei Y-C, Liu C-W, Kang W-D, Lai C-M, Tsai L-D, Wang K-W (2011) Electro-catalytic activity enhancement of Pd–Ni electrocatalysts for the ethanol electro-oxidation in alkaline medium: the promotional effect of CeO_2 addition. J Electroanal Chem 660:64–70

Wu Y, Wang D, Zhao P, Niu Z, Peng Q, Li Y (2011) Monodispersed Pd–Ni nanoparticles: composition control synthesis and catalytic properties in the Miyaura − Suzuki reaction. Inorg Chem 50:2046–2048

Xu C, Cheng L, Shen P, Liu Y (2007) Methanol and ethanol electrooxidation on Pt and Pd supported on carbon microspheres in alkaline media. Electrochem Commun 9:997–1001

Xu CW, Tian ZQ, Shen PK, Jiang SP (2008) Oxide (CeO_2, NiO, Co_3O_4 and Mn_3O_4)-promoted Pd/C electrocatalysts for alcohol electrooxidation in alkaline media. Electrochim Acta 53:2610–2618

Yang H, Wang H, Li H, Ji S, Davids MW, Wang R (2014) Effect of stabilizers on the synthesis of palladium–nickel nanoparticles supported on carbon for ethanol oxidation in alkaline medium. J Power Sources 260:12–18

Yi Q, Sun L, Liu X, Nie H (2013) Palladium–nickel nanoparticles loaded on multi-walled carbon nanotubes modified with β-cyclodextrin for electrooxidation of alcohols. Fuel 111:88–95

Yin Z, Zheng H, Ma D, Bao X (2009) Porous palladium nanoflowers that have enhanced methanol electro-oxidation activity. J Phys Chem C 113:1001–1005

Yu EH, Krewer U, Scott K (2010) Principles and materials aspects of direct alkaline alcohol fuel cells. Energies 3:1499–1528

Zhao Y, Yang X, Tian J, Wang F, Zhan L (2010) Methanol electro-oxidation on Ni@Pd core-shell nanoparticles supported on multi-walled carbon nanotubes in alkaline media. Int J Hydrog Energy 35:3249–3257

Zhao M, Abe K, Yamaura S-I, Yamamoto Y, Asao N (2014) Fabrication of Pd–Ni–P metallic glass nanoparticles and their application as highly durable catalysts in methanol electro-oxidation. Chem Mater 26:1056–1061

Zhang X, Chan SH, Ho HK, Tan S-C, Li M, Li G, Li J, Feng Z (2015) Towards a smart energy network: the roles of fuel/electrolysis cells and technological perspectives. Int J Hydrog Energy 40:6866–6919

Zhang Z, Xin L, Sun K, Li W (2011) Pd–Ni electrocatalysts for efficient ethanol oxidation reaction in alkaline electrolyte. Int J Hydrog Energy 36:12686–12697